Nuclear Materials and Energy 000 (2016) 1–7

Contents lists available at ScienceDirect

Nuclear Materials and Energy

journal homepage: www.elsevier.com/locate/nme

Optimization of mechanical alloying and spark-plasma sintering regimes to obtain ferrite–martensitic ODS steel

M.S. Staltsov[a,*], I.I. Chernov[a], I.A. Bogachev[a], B.A. Kalin[a], E.A. Olevsky[a], L.J. Lebedeva[a], A.A. Nikitina[b]

[a] National Research Nuclear University MEPhI (Moscow Engineering-Physics Institute), Kashirskoe highway 31, 115409 Moscow, Russia
[b] Joint-Stock Company VNIINM named after A.A. Bochvar, Rogova st. 5a, 123098 Moscow, Russia

ARTICLE INFO

Article history:
Received 13 November 2015
Revised 29 August 2016
Accepted 31 August 2016
Available online xxx

Keywords:
Ferritic/martensitic steel
Dispersion hardening
Mechanical alloying of powders
Spark-plasma sintering

ABSTRACT

The results of structure investigation, distribution uniformity of dispersed particles of Y_2O_3, porosity and density of the ferritic/martensitic reactor steel EP-450 (0.12C–13Cr–2Mo–Nb–V–B, wt%) produced by spark-plasma sintering (SPS) are presented. More than 140 samples were produced using different combinations of mechanical alloying (time, speed of attritor rotation) and SPS parameters (temperature, speed of reaching preset temperature, pressure and time of exposure under pressure, concentration of strengthening particles). It is determined that the absence of strengthening Y_2O_3 nano-particles in local volumes of sintered specimens is connected with the imperfection of mechanical alloying, namely, the formation of agglomerates of matrix steel powder containing no oxide nano-particles. It has been determined that the time of mechanical alloying should not exceed 30 h to provide minimum powder agglomeration, uniform distribution of Y_2O_3 particles in the powder mixture and minimum porosity of sintered samples. Spark-plasma sintering should be performed at the lowest possible temperature. As a result it was found that samples with 99% theoretical density can be obtained using the following optimized SPS-parameters: sintering temperature is 1098 ÷ 1163 K; speed for reaching the preset temperature is > 573 K/min; load is 70 ÷ 80 MPa; time of exposure under pressure – either without isothermal exposure, or exposure during ≥ 3 min; optimum quantity of Y_2O_3 is 0.2 ÷ 0.5 wt%.

1. Introduction

The main problem of achieving high-fuel burnout in fast reactors lies in the absence of radiation-resistant and at the same time heat-resistant structural materials for the active zone. With the currently achieved nuclear fuel burnout range in the reactor BN-600 of approximately 12% h.a. (about 80 dpa), the basic shell-type austenitic steel ChS-68 does not comply with requirements on radiation resistance (first of all – resistance to irradiation swelling). Intensive research and development activities are being conducted in the last decade in Russia and the world with the aim of creating chrome steel, because its irradiation swelling is much less than those of austenitic steel. The main disadvantage of chrome steel is a low heat-resistance as compared to austenitic steel when exposed to conditions occurring in active zones of fast reactors. Research focused on the creation of oxide dispersion strengthened (ODS) heat- and radiation-resistant chrome steel based on martensitic, ferritic/martensitic or ferrite structures [1–10].

One method for ODS steel creation is spark-plasma sintering (SPS) of powders which provides specific advantages (short time of obtaining high-density samples, lower temperature of compaction as compared to other methods with commensurate density and porosity parameters, relatively low applied pressure, etc.). However, this method has also a number of disadvantages: immaturity of ODS steel compaction technology; complexity of massive bodies formation on existing installations; hard and insufficient plastic compaction requiring additional thermal or any other type of processing to increase technological effectiveness of obtaining finished products, etc. [4–7].

The work in [7] shows the outcome of research on the microstructure of two ODS steels produced by hot isostatic pressing (HIP) and points out that both steels were characterized by areas without Y_2O_3 nano-particles, i.e. strengthening oxide particles in steels are distributed non-homogeneously. The authors suggested that non-homogeneous distribution of strengthening particles in

* Corresponding author.
E-mail addresses: m.staltsov@gmail.com (M.S. Staltsov), i_chernov@mail.ru (I.I. Chernov).

http://dx.doi.org/10.1016/j.nme.2016.08.020

steels can be related to an imperfection of mechanical alloying (in spite of the milling time reached up to 100 h) and HIP. With mechanical alloying of 9Cr steel powder and yttrium oxide Y_2O_3 it was established [8] that for a milling time exceeding 8 h the size of powder particles did not reduce further and according to the authors the optimum milling time is approximately 20 h. According to another data [7], the optimum time of steel powder milling is about 40 h. The work presented in [9] showed the influence of the powder shape, i.e. spherical particles or brittle flakes, on the structure of sintered samples. Furthermore, it showed that during 15 h mechanical alloying steel in the form of flakes achieved better results in terms of chemical composition and yttrium homogeneity (particles of Y_2O_3). However, during selected mechanical alloying regimes (mill rotation 400 min^{-1}, time of one milling cycle 1 h, container cooling down 1 h, total time of milling 5 and 15 h) the formation of powder agglomeration was observed, similar to the results obtained in [10]. As conclusion it was stated that the achievement of a more uniform and dispersed powder structure required an increased mechanical alloying time and optimized milling regimes.

Therefore, for obtaining high-density compacts with uniformly distributed strengthening nano-particles two steps are required: optimizing of mechanical alloying regimes (time, attritor rotation speed, elimination of powder overheating) and spark-plasma sintering in particular.

Because of that, the purpose of this work was to determine the effect of mechanical milling and SPS parameters on the uniform distribution of dispersed Y_2O_3 particles and the structure of reactor ferritic/martensitic ODS steel.

2. Materials and experimental procedure

Reactor ferritic/martensitic steel EP-450 (0.12C–13Cr–2Mo–Nb–V–B, wt%) in the form of brittle flakes after pre-milling for 2 h in a planetary ball mill MTI SFM-1 was mixed with the yttrium oxide powder. Mechanical alloying of the powder mixture was carried out in a planetary ball mill Pulverisette-5 in argon atmosphere. To ensure maximum coverage range of possible suitable sintering conditions and to receive maximum density of samples, all main parameters of the process were varied over a certain range: milling time ($\tau = 30$, 40 and 50 h), temperature (T = 1023, 1098 and 1163 K), pressure (p = 60, 70 and 80 MPa), heating rate (v = 100, 350 and 600 K/min) and isothermal exposure time under load ($\tau = 0$, 1, and 3 min). In addition, the content of Y_2O_3 changed from 0 to 1 wt % to determine the effect of steel composition on kinetics of the powder sintering.

Spark-plasma sintering was performed in the facility LABOX-625™ of Sinterland© company working in a vacuum of 5−10 Pa with a maximum pressure force up to 6 tons and power of the transmitted current up to 2500 A. Temperature was controlled by a thermocouple and infrared pyrometer. The heating of powder started out simultaneously with the application of electric current pulse and the correlated heating of the powder was done by applying pulses of 7 ms with a pause of 40 ms between pulses. There were produced more than 140 samples with dimensions of ~15 mm in diameter and 5 mm in height in various combinations of milling time and sintering parameters. The fabrication time for a specimen is 40–45 min including loading of powder and unloading of the sample.

The density and porosity of the sintered samples were measured by hydrostatic weighing using the high-precision (± 0,0002 g) analytical scale Ohaus Pioneer PA214. A scanning electron microscope (SEM) Quanta 600 FEG with energy dispersive microanalysis attachment for EDAX Trident was used to study the morphology of the powders and microstructure of sintered samples, as well as for elemental analysis. The surface structure of samples and the chemical composition of the steel after sintering were investigated at the wave Axios XRF X-ray spectrometer and SEM Zeiss EVO-50 with microprobe system. Electron microscopic studies of the fine structure of the samples were carried out in a transmission electron microscope LIBRA-120.

3. Results and discussion

Fig. 1 shows the morphology of powders with different content of Y_2O_3 after milling for 50 h. It is found that the composition of the starting powders of EP-450 steel (0.3 or 1% Y_2O_3) does not affect the size of the activated particles, the degree of homogeneity of milling and powder agglomeration. Despite the use of previously established optimized regimes of mechanical alloying (Table 1), after milling for 30 h the powder agglomerates still had a maximum size up to 30 µm. With increasing milling time to 40 and 50 h the degree of agglomeration practically did not change compared to milling for 30 h, but the uniformity of powder slightly increased.

As shown by the work done in [9], after milling for 15 h the distribution of Y_2O_3 oxide in powder is already quite homogeneous and its content practically complies with a target one. The yttrium distribution determined via SEM showed that after 30 h of milling Y_2O_3 oxide was distributed completely uniformly on the steel powder surface (Fig. 2). Therefore, from the perspective of minimum agglomeration and Y_2O_3 oxide distribution homogeneity in the powder 30 h of mechanical activation is found to be an optimum.

Fig. 3(a) shows the general view of the sintered steel structure with 1 wt% Y_2O_3, where ferrite and martensitic grains are observed. The area with oxides is represented in Fig. 3(b). Microstructure in Fig. 3 contains large particles being the $M_{23}C_6$ type carbides, yttrium oxides with a maximum size of the oxide particles up to 40 nm and double oxides of yttrium and silicon. Silicon oxide was found in the work [10] as well.

In general, the microstructure of the surface of sintered samples is quite homogeneous. However, local areas provide a specific structure which is exemplarily shown in Fig. 4. One can see a large elongated grain situated in a highly dispersed structure that formed from a powder agglomerate during the SPS process. The grain orientation corresponds to the direction perpendicular to the sample pressing axis. Such grains are consisting of smaller equiaxial grains with the size 5 ÷ 7 µm (Fig. 5) formed from steel powders being a part of the agglomerate. Such substructure is characteristic for all grains formed from powder agglomerates. Fig. 4 shows open porosity along boundaries of small grains, while a large grain formed from the powder agglomerate shows no porosity. With the increase of mechanical alloying time from 30 to 40 and 50 h the porosity increases.

Chemical composition of different areas of sample with 0.3 wt% of Y_2O_3 is shown in Table 2. Analysis of Fig. 4 and data in Table 2 shows that in view of the main elements the compact complies with the composition of matrix steel. In spectrum 2 an increased content of Si, O are observed and with the presence of Y the formation of double yttrium and silica oxides can be deduced. The content of yttrium of approximately 0.18 wt% corresponds to the content of 0.3 wt% Y_2O_3, that was introduced into steel. In spectrum 1 taken from the large grain formed from the agglomerate, no yttrium was found.

Accordingly, above results verify that in case of powder agglomerates formation in the process of mechanical alloying, grains formed from these agglomerates during the subsequent SPS process do not contain yttrium (yttrium oxide) or at least do not contain it in sufficient quantity for experimental detection. Data received about the inhomogeneity of oxide particles in ODS steels produced by SPS were similar to results of HIP produced materials obtained in the work [7].

Please cite this article as: M.S. Staltsov et al., Optimization of mechanical alloying and spark-plasma sintering regimes to obtain ferrite–martensitic ODS steel, Nuclear Materials and Energy (2016), http://dx.doi.org/10.1016/j.nme.2016.08.020

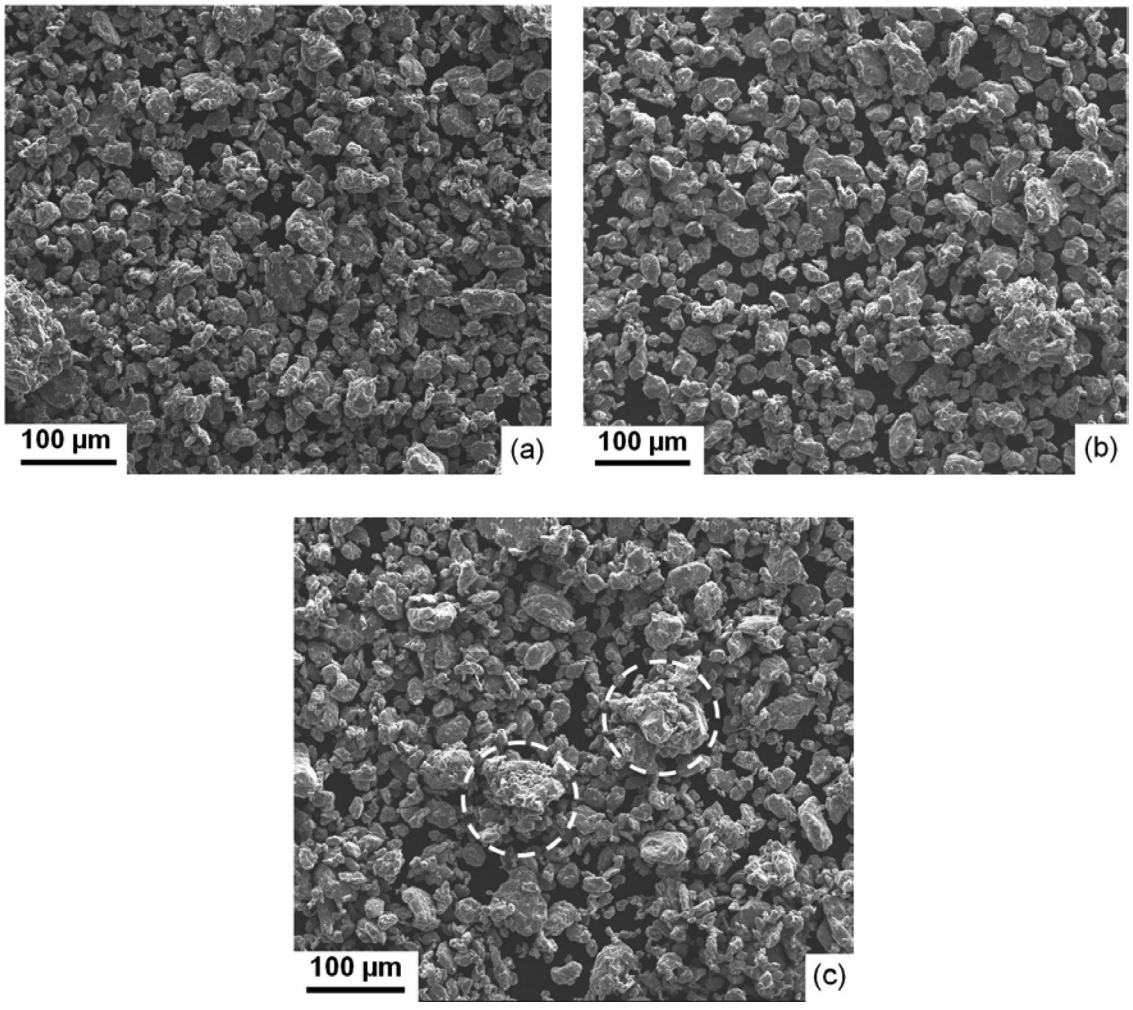

Fig. 1. Morphology of steel powder with 0.3% Y_2O_3 (a) and 1% Y_2O_3 (b) after mechanical alloying for 50 h; powder agglomerates are marked by circles (SEM).

Table 1
Optimized regimes of mechanical alloying of powders of steel EP-450 and oxide Y_2O_3.

The time of one cycle of milling, h	Container cooling time, h	Number of turns of the mill, min^{-1}	The atmosphere	The total time of milling, h
2	1	200	Ar (99.99%)	30, 40 and 50

Table 2
Chemical composition (0.3 wt% Y_2O_3) of ODS steel obtained in EVO-50 by electron beam scanning of areas 1 and 2.

Element	Content, wt%		
	Spectrum 1	Spectrum 2	Standart deviation
Fe	82.76	80.88	0.99
Cr	13.94	14.37	0.26
Si	0.28	0.54	0.13
Mn	0.63	0.66	0.11
Ni	0.24	0.33	0.05
Mo	1.46	1.52	0.03
Nb	0.31	0.28	0.03
V	0.20	0.25	0.04
Y	0.00	0.18	0.11
O	0.18	0.99	0.40

The study of strengthening particles concentration influence on EP-450 ODS steel sintering aims at a better understanding of the processes occurring during sintering and, possibly, helps selecting the optimum concentration of yttrium oxide in the steel in terms of material compaction. For this purpose, sintering was conducted without and with 0.3 wt% of Y_2O_3 at two pressures, i.e. 70 and 80 MPa (Fig. 6). The results show that the pressure practically does not have an influence on the steel powder sintering without Y_2O_3, while the density of those samples with Y_2O_3 increases insignificantly with the pressure rise from 70 to 80 MPa. At the same time, addition of 0.3 wt% of Y_2O_3 results in a reduction of the sintering speed and lower finished sample density. This is related to the fact that Y_2O_3 particles prevent sticking of steel particles and sinter with each other worse at such temperatures due to their hard-melting nature.

In this connection, the direct influence of different concentrations of hard-melting inclusions on material sintering kinetics is of high interest. For that purpose, experiments were conducted with regard to steel sintering of 6 different concentrations of Y_2O_3 – 0.15, 0.2, 0.3, 0.4, 0.7 and 1.0 wt%. Data of samples compaction speed with different Y_2O_3 content shown in Fig. 7 indicate that with the increase of yttrium oxide concentration up to 0.3 wt% considerable growth of compaction speed is observed, while a further increase of Y_2O_3 content reduces the compaction speed. Therefore, non-linear dependence is observed of EP-450 ODS steel

Please cite this article as: M.S. Staltsov et al., Optimization of mechanical alloying and spark-plasma sintering regimes to obtain ferrite–martensitic ODS steel, Nuclear Materials and Energy (2016), http://dx.doi.org/10.1016/j.nme.2016.08.020

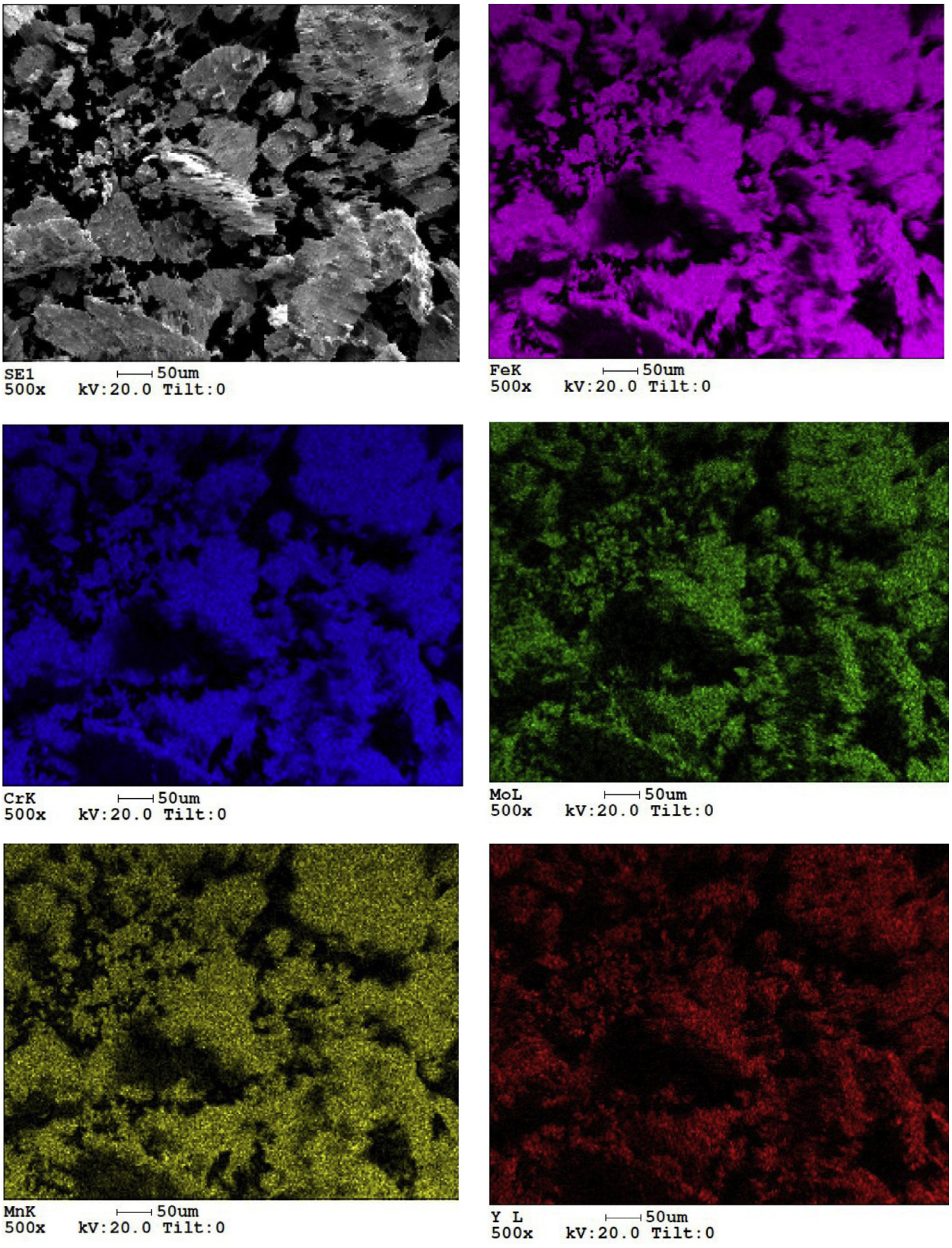

Fig. 2. Distribution map of some components of steel (Cr, Mo, Mn) and Y (Y_2O_3) in a powder mixture of steel EP-450 + 1% Y_2O_3 after milling for 30 h.

Please cite this article as: M.S. Staltsov et al., Optimization of mechanical alloying and spark-plasma sintering regimes to obtain ferrite–martensitic ODS steel, Nuclear Materials and Energy (2016), http://dx.doi.org/10.1016/j.nme.2016.08.020

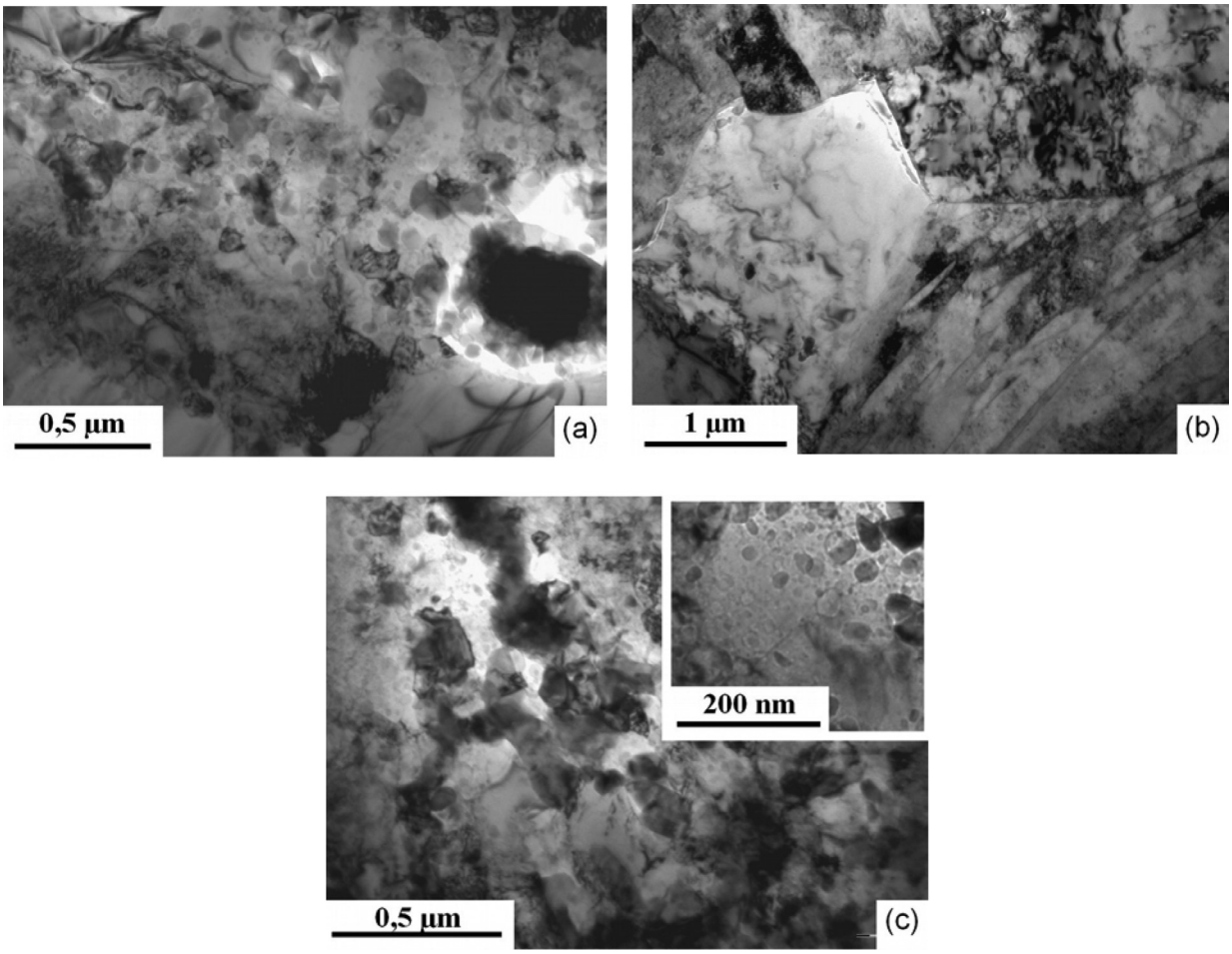

Fig. 3. A general view of the structure of the sintered steel with 1 wt% Y_2O_3 with ferritic and martensitic grains (a) and the area with oxides particles (b) (TEM).

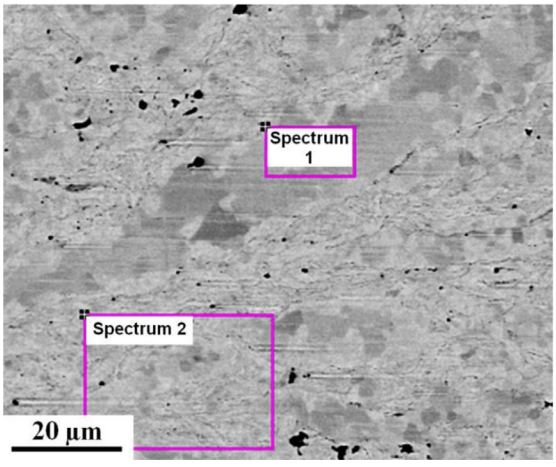

Fig. 4. Microstructure of the sample surface of steel with 0.3 wt% Y_2O_3 (SEM).

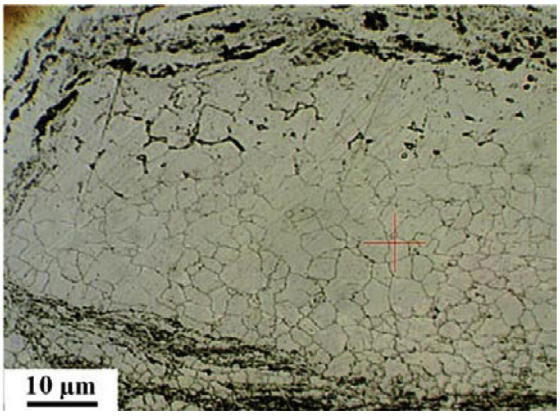

Fig. 5. The substructure of grains formed from steel powder agglomerate.

compaction speed from concentration of Y_2O_3 at spark plasma sintering.

Fig. 8 shows the dependence of the relative density of sintered samples on the time of mechanic alloying, applied pressure and temperature of sintering. One can see that at all used milling times and pressures a temperature of 1023 K is evidently not sufficient to obtain highly compacted samples. When the temperature increases up to 1098 and 1163 K the density of sintered samples increases considerably, with the largest values being observed at p = 70–80 MPa independent on the time of mechanical activation. As can be seen in the Fig. 8(a), at mechanical alloying of powders with 0.3 wt% of Y_2O_3 during 30 h and a pressure of 70 and 80 MPa during SPS the density of compacts achieves a maximum of approximately 99% theoretical density. At the same time, as shown in Fig. 8, at identical conditions of mechanical milling and SPS the density of steel with 1 wt% of Y_2O_3 is considerably lower than of compacts with 0.3 wt% of Y_2O_3 and even in the best case does not exceed 97%. Porosity increase accompanied by density decrease with the milling period occurring from 30 to 40 and 50 h can be

Please cite this article as: M.S. Staltsov et al., Optimization of mechanical alloying and spark-plasma sintering regimes to obtain ferrite–martensitic ODS steel, Nuclear Materials and Energy (2016), http://dx.doi.org/10.1016/j.nme.2016.08.020

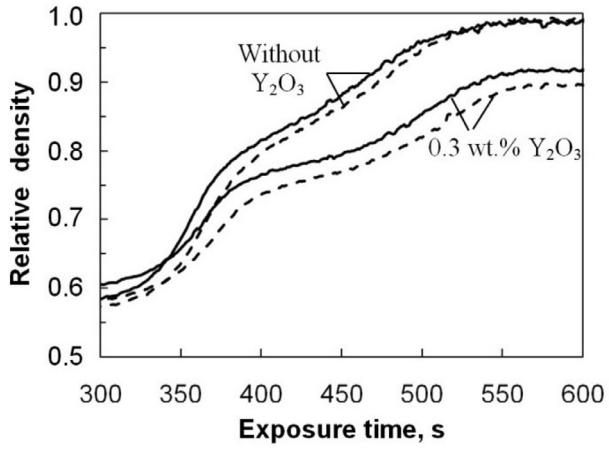

Fig. 6. The relative density of the samples during sintering of steel powder without Y_2O_3 and with 0.3 wt% Y_2O_3 for p = 70 MPa (- - - -) and 80 MPa (——); milling for 30 h, T = 1163 K, v = 100 K/min, τ = 1 min. The entire sintering process is shown from the moment the pulses of electric current turn on to their switching off.

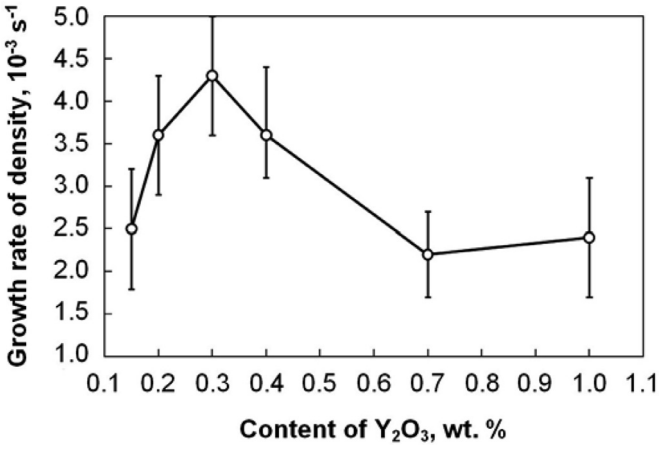

Fig. 7. Density increasing kinetics depending on the Y_2O_3 concentration under sintering conditions: p = 80 MPa, T = 1163 K, v = 100 K/min τ = 1 min.

connected with the fact that fractions of nanosized particles (especially in the range of 1–10 nm) formed during long time milling have much lower melting temperature [11,12] and in the aggregate form most models are described by the equation $T_m(r) = T(1-a/r)$.

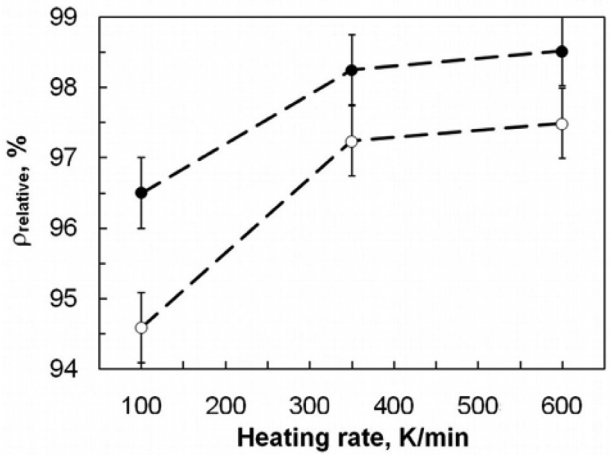

Fig. 9. Relative density of the samples with 0.3 wt% Y_2O_3 (●) and 1 wt% Y_2O_3 (○) depending on heating rate up to a temperature of 1163 K (milling time is 30 h, p = 70 MPa, τ = 1 min).

Table 3
The isothermal exposure time dependence of relative density of samples with 1 wt% Y_2O_3 during sintering at T = 1163 K, P = 70 MPa, v = 100 °C/min.

τ, min	0	1	3
$\rho_{relative}$, %	96.9 ± 0.5	94.9 ± 0.5	96.4 ± 0.5

Increasing of milling time above 30 h does not only result in further powder refinement, but also the powder grain size does not reduce.

Moreover, at selected pressure and temperature of sintering there are certain possibilities to reduce porosity and, accordingly, to increase density of sintered samples. This is done by means of heating speed change (Fig. 9) and change of the exposure time under pressure (Table 3) in the SPS process.

Based on the dependencies shown in Fig. 9, a conclusion can be drawn that heating speed increases the finished density of samples. Most likely, this effect occurs due to higher current intensity flowing through the sample in order to provide higher heating speed which causes more intensive generation of Joule heat in inter-particle contacts and results in their better adhesion to each other. In order to obtain the maximum density, the heating speed should, at least, exceed 300–400 K/min. Moreover, as shown in Fig. 9, in identical sintering conditions samples with 0.3 wt% of

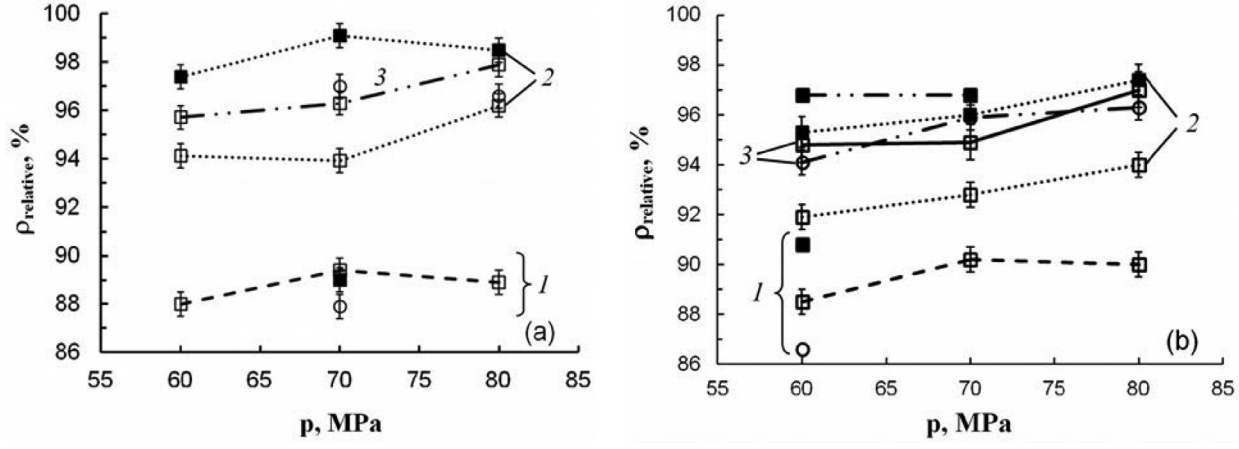

Fig. 8. The relative density of the samples as a function of applied pressure at sintering temperature 1023 (*1*), 1098 (*2*) and 1163 K (*3*) for powders with 0.3 wt% Y_2O_3 (a) and 1 wt% Y_2O_3 (b) mechanically alloyed during 30 (■), 40 (□) and 50 h (○), v = 100 K/min, τ = 1 min.

Please cite this article as: M.S. Staltsov et al., Optimization of mechanical alloying and spark-plasma sintering regimes to obtain ferrite–martensitic ODS steel, Nuclear Materials and Energy (2016), http://dx.doi.org/10.1016/j.nme.2016.08.020

Y_2O_3 become more dense than with 1 wt% of Y_2O_3 which is in conformity with the data shown in Fig. 8.

Results in Table 3 show that 1 min exposure under pressure causes a reduction of relative density as compared to sintering without it. Furthermore, density values at exposure increasing up to 3 min rise again to practically the same values that had been observed during sintering without isothermal exposure under pressure. The observed dependency shown in the Table 3 indicates that some processes are occurring in the material at constant temperature with the change of exposure time under pressure. For example, EP-450 steel after standard heat thermal (normalization from 1373 K + high tempering at 993 K) consists of two-phases (ferrite grains and tempered martensite – sorbite). However, when the temperature rises up to 1163 K less temperature resistant chromium carbide and vanadium carbide decay, former sorbitol grains are supersaturated with carbon, and at a certain temperature in these areas an $\alpha \rightarrow \gamma$-transformation is possible [1,13]. In the exposure process during 1 min, when the relaxation of the structural-phase condition occurs, a number of competing processes are possible: nucleation of secondary phases, coagulation of second phase particles, and further dissociation of carbides that results in the decrease of the compact density. A subsequent increase of the compact density after three-minute exposure at 1163 K is a consequence of additional compaction of powder filling under the influence of applied pressure. However, processes occurring at high temperature and depending on the powder exposure time under pressure can be even more complicated. Accordingly, a final explanation of such dependence of compacts density on exposure time is difficult and requires further research of the obtained phenomenon. However, it should be noted that the dependence of ρ_{relative} on exposure time shown in the Table 3 is reproducible and is characteristic for all spark-plasma sintering parameters under consideration.

4. Conclusions

It is found that the absence of hardening Y_2O_3 nanoparticles in local volumes of ODS steels is due to the imperfection of the mechanical alloying process, namely the formation of steel powder agglomerates without oxide nanoparticles in the internal volume during mechanical alloying.

It has been shown that mechanical alloying time should not exceed 30 h to provide mini- mum powder agglomeration, uniform distribution of the Y_2O_3 oxide in the powder mixture and minimum porosity of compacts.

It has been established that due to melting of the nanosized powder fraction and the related formation of an open porosity at the grain boundaries, SPS should be carried out at the lowest possible temperature.

For the fabrication of ODS EP-450 steel of minimum porosity and maximum density the optimal parameters of mechanical alloying and spark-plasma sintering are:

- time of 1 milling cycle is 2 h;
- cooling time of container is 1 h;
- number of turns of the mill is 200 min^{-1};
- total time of milling is 30 h;
- optimum amount of Y_2O_3 is $0.2 \div 0.5$ wt%;
- the heating rate to a predetermined temperature is > 300 K/min;
- pressure is $70 \div 80$ MPa;
- exposure time under load is 0 or ≥ 3 min;
- sintering temperature is $1098 \div 1163$ °C.

Acknowledgement

The work was carried out within the scope of Center of Nuclear Systems and Materials under Governmental Support of Competitive Growth Program of NRNU MEPhI (agreement with the Ministry of Education and Science of the Russian Federation dated August 27, 2013 No.02.a03.21.0005), implementation of state assignment in the sphere of scientific activities №3.483.2014/K dated 10.06.2014.

References

[1] B.A. Kalin, P.A. Platonov, Yu.V. Tuzov, I.I. Chernov, Ya.I. Shtrombah, Physical Materials Science, vol. 6, Structural Materials for Nuclear Technology, MEPhI, Moscow, 2012 (in Russian).
[2] S. Ukai, M. Fujiwara, J. Nucl. Mater. 307–311 (2002) 749–757.
[3] V.S. Ageev, A.A. Nikitina, V.V. Sagaradze, Problems At. Sci. Technics. Ser.: Radiat. Damage Phys. Radiat. Mater. Sci. 2 (90) (2007) 134–141 (in Russian).
[4] Y. Xu, Z. Zhow, M. Li, J. Nucl. Mater. 417 (2011) 283–285.
[5] Cs. Balazsi, F. Gillemot, M. Horvath, et al., J. Mater. Sci. 46 (2011) 4598–4605.
[6] S.K. Karak, J. Dutta Majumdar, W. Lojkowski, et al., Phil. Mag. 92 (5) (2012) 516–534.
[7] Dai Lei, Liu Yongchang, Ma Zongqing, et al., J. Mater. Sci. 48 (2013) 1826–1836.
[8] Lu Chen-yang, Lu Zheng, Liu Chun-ming, J. Nucl. Mater. 442 (2013) S148–S152.
[9] I.I. Chernov, M.S. Staltsov, B.A. Kalin, et al., Atomic Energy 116 (1) (2014) 42–47.
[10] P. Olier, M. Couvrat, C. Cayron, et al., J. Nucl. Mater. 442 (2013) S106–S111.
[11] O. Koper, S. Winecki, Specific heats and melting points of nanocrystalline materials, in: K.J. Klabunde (Ed.), Nanoscale Materials in Chemistry, John Wiley & Sons, Inc, New York, USA, 2001, pp. 263–277.
[12] A.V. Fedorov, A.V. Syul'gin, Mathematical modeling of metal nanoparticles melting, Novosibirsk, S.A. Christianovich Institute of Theoretical and Applied Mechanics of Siberian Division of the Russian Academy of Sciences, 2012, p. 23–29 (in Russian).
[13] M. Yamamoto, S. Ukai, S. Hayashi, J. Nucl. Mater. 417 (2011) 237–240.

Please cite this article as: M.S. Staltsov et al., Optimization of mechanical alloying and spark-plasma sintering regimes to obtain ferrite–martensitic ODS steel, Nuclear Materials and Energy (2016), http://dx.doi.org/10.1016/j.nme.2016.08.020